

TABLE 2. Spectroscopic characteristics in the red.

Name MBG	V_r km s ⁻¹	[OI] 6300	[NII] 6583	[SII] 6716	[SII] 6730	$-\log I_{H_\alpha}$ (ergs cm ⁻² s ⁻¹)	FWHM H _α km s ⁻¹	EW H _α (Å)
02384-2112	4712	...	0.42	13.39	141	20
03196-1939	4076	...	0.27	0.20	0.16	13.09	32	49
03288-1448	9234	...	0.34	0.13	0.12	13.58	99	31
03325-1002	9596	0.28	0.40	0.10	0.11	12.70	148	65
03537-1351	8891	...	0.84	13.42	264	37
23362-0448	5990	...	0.43	0.11	0.11	13.39	117	17

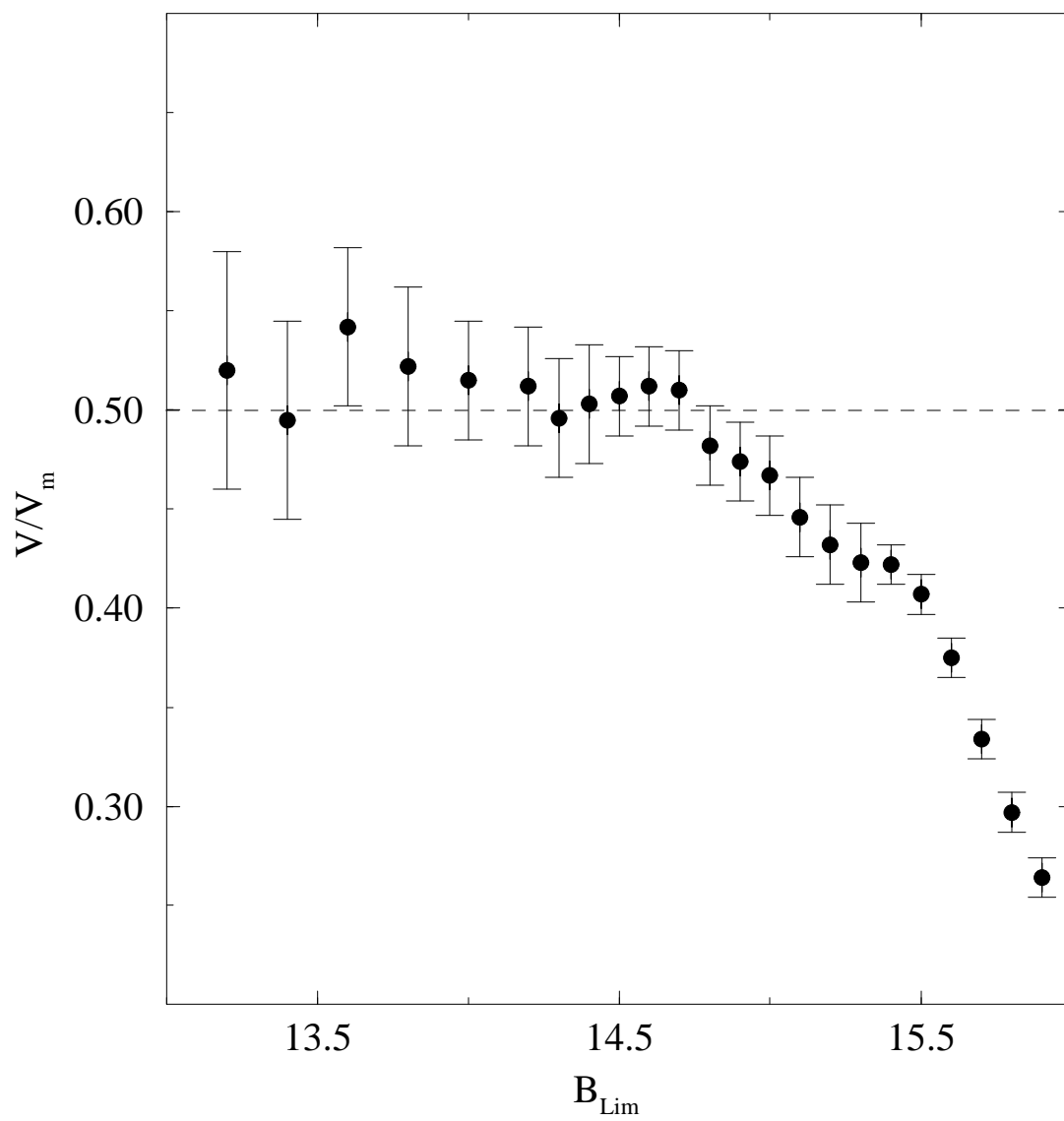


TABLE 3. Spectroscopic characteristics in the blue.

Name	[OIII] 4959	[OIII] 5007	$-\log I_{H\beta}$ (ergs cm ⁻² s ⁻¹)	FWHM H _{β} km s ⁻¹	FWHM [OIII] λ 5007 km s ⁻¹	EW H _{β} (Å)
01325–1806	...	0.46	13.9	112	151	6
01486–0956	...	0.41:	14.2:	< 296	< 354	3
01556–2002	...	2.53:	14.4:	< 314	< 348	5
02027–2339	1.36	3.78	14.7	187	< 438	16
02028–0641	...	0.3	13.6	370	218	9
02399–2420	0.69:	1.69:	14.0:	< 339	< 294	8
02384–2112	...	1.57	14.4	< 401	< 425	3
03325–1002	0.11	0.32	13.6	154	72	10
03353–2439	...	0.42	13.6	171	< 480	9
03424–2019	0.16	0.40	14.9	< 419	< 384	8
04002–1811	0.94	2.81	14.0:	230	306	4
21481–1330	0.33:	0.69	13.8	300	187	10
21300–1601	0.15	0.46	13.9	< 413	< 455	14
22342–2228	2.17	5.75	14.1	990	218	4
23318–1156	0.80	2.18	14.1	112	< 413	5
23383–1921	1.09	3.49	13.4:	278	< 467	23
23382–2047	0.18	0.69	13.8	311	271	7

Uncertainties higher than 20% are marked by a colon.

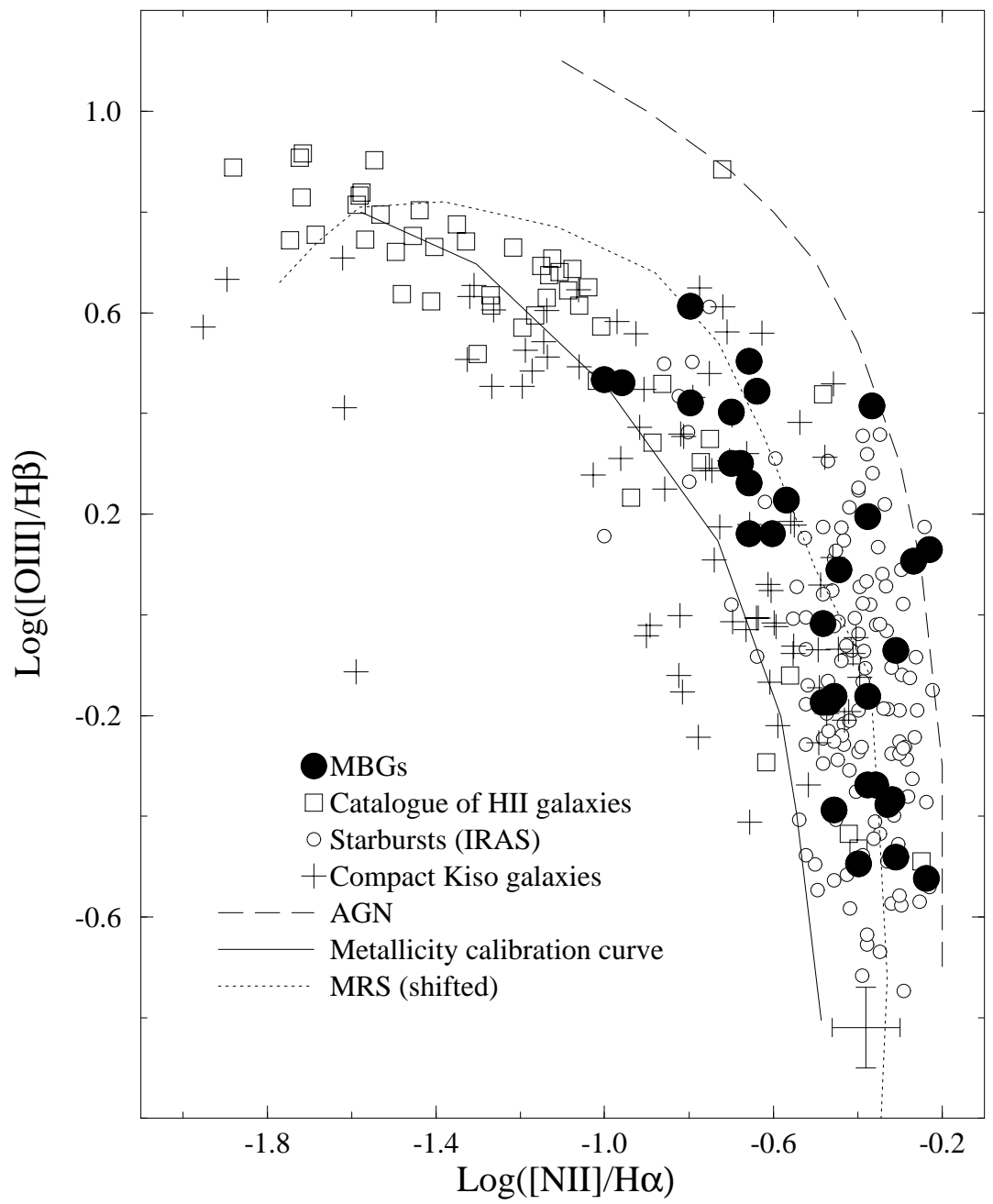


TABLE 4. Metallicities and electron densities of selected MBGs

Name	logO/H	n(e) cm ⁻³
00086-1223	8.2	280
01320-1604	8.6	...
01325-1806	9.0	...
01486-0956	9.0	200
01556-2002	8.4	< 100
01166-1719	...	< 100
02028-0641	> 9.0	< 100
02384-2112	8.6	...
02399-2420	8.6	100
03196-1939	...	120
03288-1448	...	320
03325-1002	> 9.0	630
03353-2439	9.0	630
04054-2133	...	200
21300-1601	9.0	< 100
21481-1330	8.8	...
22342-2228	8.3	...
23362-0448	...	450
23382-2047	8.8	280

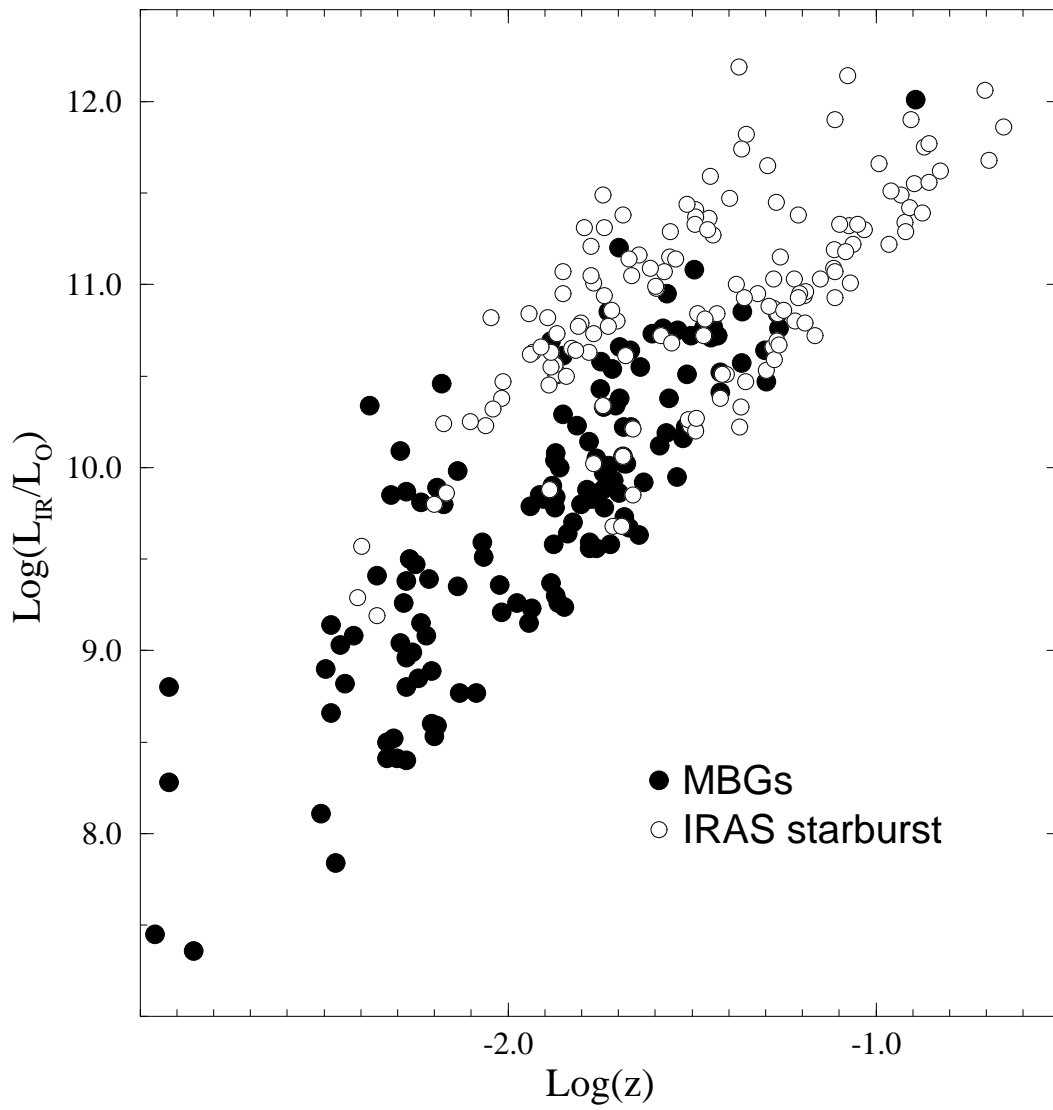
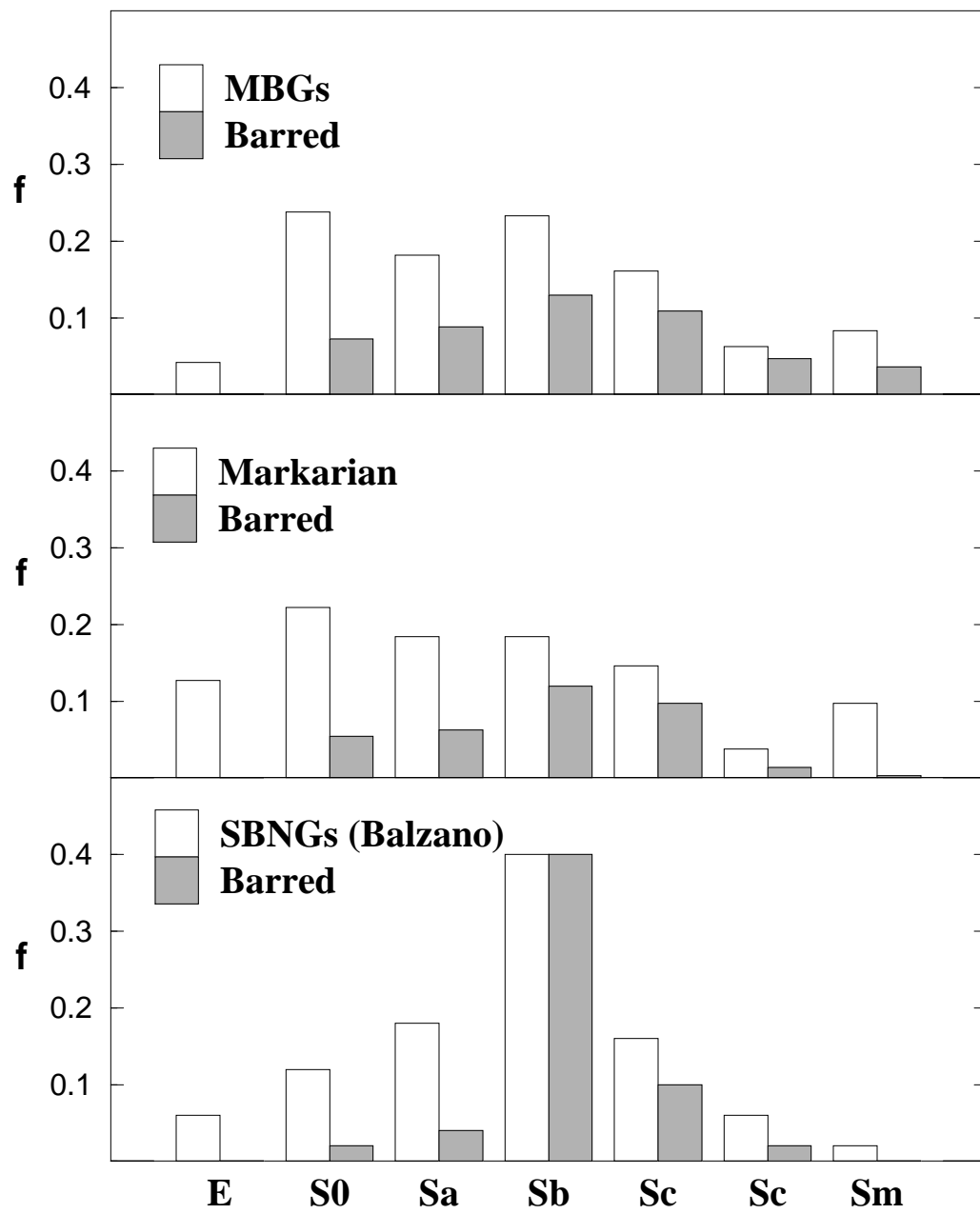


TABLE 5. CCD photometry of selected MBGs

MBG	B_T	V_T	R_V (arcsec)	B-V
22066-2539	14.97	14.29	30	0.68
23166-2255	14.34	13.79	60	0.55
23372-2301	14.68	14.13	30	0.55
23387-1514	15.68	15.28	12	0.40
00027-1645	14.40	13.81	30	0.59
00085-1223	14.02	13.33	35	0.69
00129-2143	13.52	12.69	80	0.83
00142-0532	14.08	13.37	45	0.71
00287-1045	14.86	14.62	35	0.24
00376-2020	14.62	14.24	35	0.38
00392-1707	14.52	13.89	50	0.63
00439-1342	13.65	13.00	50	0.65
00524-1655	15.64	15.17	12	0.47
01053-1746	13.47	13.07	40	0.40
01359-2310	15.40	14.68	16	0.72
01386-0549	13.97	13.30	60	0.67
01428-0404	14.94	14.18	40	0.76
02010-1010	14.60	14.07	35	0.53
02062-0801	13.85	13.33	50	0.52
02141-1134	13.72	12.62	40	1.10
02358-1601	14.14	13.68	30	0.46
02411-1457	13.30	12.59	50	0.71
02557-1033	14.10	13.56	30	0.54
03083-1059	15.02	14.32	30	0.70
03154-0728	13.43	12.94	40	0.49
03312-1818	13.71	13.14	45	0.57
03324-1000	13.78	13.04	30	0.74
03491-1533	14.29	13.80	35	0.49



The Montreal Blue Galaxy Survey III.

Third list of UV-bright candidates¹

Roger Coziol²

Instituto Nacional de Pesquisas Espaciais (INPE), Divisão de Astrofísica
Caixa Postal 515, 12201/970 Sao Jose dos Campos, SP, Brazil.

Serge Demers² and Rémi Barnéoud

Département de Physique, Observatoire du Mont Mégantic
Université de Montréal, Montréal, Québec, H3C 3J7 Canada

and

Miriam Peña

Instituto de Astronomia, Universidad Nacional Autónoma de México
Apdo. Postal 70-264, 04510 México D. F., México

Received _____; accepted _____

¹ Partially based on observations obtained at Observatorio Astronómico Nacional, San Pedro Mártir, B. C., México.

²Visiting Astronomer, Cerro Tololo Inter-American Observatory. CTIO is operated by AURA, Inc. under contract to the National Science Foundation.

ABSTRACT

We present and discuss the latest addition of the Montreal Blue Galaxy (MBG) survey. Inspection of 59 Curtis Schmidt plates resulted in the identification of 135 new UV-bright galaxies with $B < 15.5$. This brings the total number of MBGs to 469. New results of the V/V_m test show that our survey is complete to $B = 14.7$.

From our most recent spectroscopic follow-up, we confirm the discovery of one new Seyfert 1 galaxy and possibly one new Seyfert 2 galaxy. We confirm also the bias of the MBG survey towards the low-excitation and metal rich Starburst Nucleus Galaxies (SBNGs). The spectral characteristics of the MBGs are similar to those of the infrared luminous IRAS galaxies. As a common characteristic, they show a mean ratio $\text{Log}([\text{NII}]/\text{H}\alpha)$ in excess of 0.2 dex as compared to normal disk HII regions. In general, the MBGs have lower far-infrared luminosities ($L_{IR} < 10^{11} L_{\odot}$) and are nearer ($z < 0.05$) than the luminous IRAS galaxies.

The distribution of the morphologies of the MBGs indicates a high number of early-type spirals (Sb and earlier). Nearly half of these galaxies also possess a bar. In our sample, the fraction of galaxies with bars depends on the morphology and increases towards the late-type spirals. However, if we consider only isolated galaxies, the late-type spirals show a clear tendency to be barred. Signs of a recent interaction with neighbor galaxies are obvious only in 24% of our candidates. Although this number is only a lower limit, it is nevertheless sufficiently low to suggest that in a majority of massive galaxies the burst of star formation do not depends solely on dynamical processes.

1. INTRODUCTION

This article is the third of a series of papers presenting and discussing the results of the MBG survey. The aim of our project is to increase substantially the number of known UV–bright galaxies in the south galactic pole area. In parallel with our main effort, spectroscopic and imaging programs have also been implemented to determine the nature of our candidates and identify the origin of their activity. From spectroscopy, we determined that 95% of the MBGs are starburst galaxies (Coziol *et al.* 1993, hereafter Paper I). Comparison of the MBGs properties with those of galaxies found in other surveys (Coziol *et al.* 1994, hereafter Paper II) suggested that our survey is biased towards the low-excitation Starburst Nucleus Galaxies (SBNGs). In general, the SBNGs are more massive and more chemically evolved than the high excitation HII galaxies (Salzer *et al.* 1989; Terlevich *et al.* 1991).

The mechanism responsible for the starburst phenomenon is still unknown (see Gallagher [1993] for a brief discussion of possible alternatives). For the massive SBNGs, it is usually believed that they are evolved galaxies which were rejuvenated by a recent infall of matter (Huchra 1977). It is also believed that this new injection of matter is related to some kind of interaction with another galaxy. To verify this hypothesis, we have taken CCD images of a sub–sample of the MBGs (Coziol *et al.* 1995; Barth *et al.* 1995). Although many of these galaxies are clear examples of interacting or merging galaxies, almost half are relatively isolated. A more complete analysis of our images further revealed that all the isolated galaxies present peculiar morphological characteristics that could be interpreted as indirect signs of interactions. These galaxies could be remnants or advanced stages of past interacting galaxies (Barth *et al.* 1995). But this would also imply that the present burst of star formation in these galaxies is somehow decoupled from the presumed triggering event (Coziol *et al.* 1995). Confirmation of this behavior for a larger number of SBNGs would

suggest that in some of the massive starbursts the star formation process may depend on internal as well as external causes.

Our third addition increases by $\sim 40\%$ the number of MBGs. This allows us to better define the global properties of our candidates and verify some of the results presented in our previous papers. The plan of this article is the following. The third list is described in section 2. The results of our last spectrophotometry follow-up are presented in section 3. New photometric observations of bright candidates are described in section 4. We rediscuss the completeness limit of our survey in section 4. In section 5, we conclude with a brief discussion on the possible causes at the origin of the bursts in our candidates.

2. THE THIRD LIST OF MBG CANDIDATES

The third list of 135 MBG candidates ensues from the inspection of a set of 59 plates, corresponding to an area of 1376 deg^2 . This third installment brings the level of completion of our survey to 63%, and reaches now 4400 deg^2 . Information on the new candidates identified is compiled in Table 1. It follows the same format used in the previously published tables. The name of the object is based on its 1950 equatorial coordinates. The calibrated photographic B magnitudes and U–B colors are obtained from the APM measurements. As determined in Paper I, the mean uncertainty of the B_{APM} is ± 1 magnitude. It is important to remember that the machine determined U–B color is not a reliable indication of the true color (see Paper I). It is included in our list only for the sake of completeness. Absolute magnitudes are estimated using the B_{APM} and the radial velocity given by the NASA/IPAC Extragalactic Database (NED), assuming $H_0 = 75 \text{ km s}^{-1} \text{ Mpc}^{-1}$. Uncertainties for the coordinates are of the order of arcseconds. Other information found in Table 1 are cross-identification with objects found in NED. An “n” in the last column refers to a note in the Appendix. In this third list, several galaxies were not found in the APM file of the

particular Schmidt plate. Because of some peculiarities in their images, the APM machine ignored those objects. We include them in our list, because they represent good UV-bright candidates. In Table 1, those few cases are identified by a “*”. For these galaxies, we quote the B magnitude and coordinates as found in NED.

The total list of MBGs amounts to 469 galaxies brighter than $B_{APM} = 15.5$. It corresponds to a density of 0.11 galaxy per deg^2 . This is almost the density of galaxies found by the Markarian survey (Mazzarella & Balzano 1986). By comparison, the densities of galaxies found in the Kiso (Comte *et al.* 1994) and the Northern Case surveys (Salzer *et al.* 1995) represent 15 times and 13 times the density per deg^2 of the MBG survey. These differences are explained by the fact that these two surveys go at least one magnitude deeper than the MBG survey ($B \sim 16.5$).

A fraction of the fields covered by the Kiso survey are located south of the celestial equator. Because the Kiso magnitudes are roughly similar to those of the APM, we can arbitrarily assign a magnitude limit to this survey and compare some of their output to our results. Using the lists of Takase & Miyauchi-Isobe (1993), we determined that 96 Kiso UV-bright galaxies (or KUGs), with an apparent magnitude brighter or equal to $B = 15.5$, are located in the area overlapping with our 187 fields. Only $\sim 20\%$ of these galaxies are included in our 3 lists. We note that in the Kiso survey the degree of UV-excess of the KUGs is coded H, M and L, corresponding to high, medium and low. The MBGs include 12 out of the 66 (18%) KUGs marked L, 5 out of the 24 (21%) marked M, and 5 out of the 6 (83%) marked H. Contrary to the Kiso survey, we do not try to establish any gradation in the level of UV-excess of our candidates. Therefore, the MBG Survey detects essentially all of the strongest UV-excess objects, but relatively few of the intermediate and low UV-excess galaxies. This comparison suggests that the MBG selection criterion is more restrictive than that used by the Kiso survey.

3. SPECTROPHOTOMETRY

3.1. *Data acquisition*

Spectrophotometric observations of a sample of 22 galaxies were obtained with the 2.1 m telescope located at the Observatorio Astronómico Nacional, San Pedro Mártir, B. C., México, during 4 nights in October 1993. The configuration of the instruments was exactly as described in Paper II. A Boller & Chivens spectrograph, equipped with a blue coated, 1024×1024 Thompson CCD detector was employed. We used two gratings of 600 lines/mm (blazes 13 and 8.63 degrees) to obtain red (5800–7200 Å) and blue (4400–5900 Å) spectra of the candidates. All the observations were made with the slit centered on the nucleus of the galaxy, oriented E-W, and a slit width of 150 and 250 μm , corresponding to 2.0 and 3.3 arcseconds in the sky. For each galaxy, we obtained two spectra in the red (10 min. exposure time) and two in the blue (20 min. exposure time). The mean resolution is 4 Å in the red and 8 Å in the blue. A He-Ar lamp was used for wavelength calibration. Flux calibration was provided by additional observations of standard stars from the lists of Stone (1977), Stone & Baldwin (1983) and Baldwin & Stone (1984). Due to poor weather conditions, the fluxes measured during the first night of observation are poorly determined. Uncertainties of the fluxes for this night are higher than 20%. For data reduction, we have followed the same procedures as described in Paper I and Paper II.

3.2. *Data analysis*

One of our goals during our most recent observing run at San Pedro Mártir was to complete the observations made during the previous missions. We therefore reobserved in the blue almost all of the galaxies for which we already had a red spectrum. Only 6 new galaxies were observed in the red. The results are presented in Tables 2 and 3. In Table 2,

the intensities of the lines are given relative to $H\alpha$. In Table 3 they are given relative to $H\beta$. As in the two previous papers, the lines were measured by adjusting gaussian fits to the profiles, setting the continuum by eyes. No correction for galactic interstellar reddening or intrinsic reddening has been applied. The uncertainties on the fluxes are of the order of 10%, and represent the internal consistency of our method only. It was determined by comparing the values measured on two different (independent) spectra of the object. In Table 2, the radial velocities were derived from the average of the detected lines, but were not corrected for the Earth motions. Uncertainties for the radial velocities are of the order of 60 km s^{-1} . Also listed in Tables 2 and 3 are the full width at half maximum (FWHM), corrected for the instrument profile, and the equivalent width (EW) of $H\alpha$ and $H\beta$.

In Fig. 1, we show the spectra of MBG22342-2228 which was classified in Paper II as a possible AGN. The additional blue spectrum allows us to classify this galaxy as a Seyfert 1. Fig. 2 shows the available red spectrum of MBG03536-1351. The $[\text{NII}]\lambda 6584/H\alpha$ ratio is high suggesting that it could be another AGN. Based on the absence of a wide component for the $H\alpha$ line, we tentatively classified this galaxy as a Seyfert 2. Observation in the blue part of the spectrum will be necessary to confirm this classification. Our current yield of AGNs implies that barely 5% of our galaxies will be of this nature.

As in Paper II, we have estimated the metallicity of our candidates using the diagnostic diagram $[\text{OIII}]\lambda 5007/H\beta$ vs. $[\text{NII}]\lambda 6584/H\alpha$. Our method is based on the calibration of this diagram using a sample of galaxies from the literature for which reliable chemical abundances exist (see Paper II). The uncertainty associated with our method is approximately 0.3 dex. The estimated metallicities for 19 MBGs are presented in Table 4. In this table, we give also the electron densities of some of the galaxies. These densities were estimated using the sulfur doublet $[\text{SII}]\lambda\lambda 6716,6717$, assuming for the ionized gas an electron temperature of 10 000 K. Both the metallicities and electron densities are typical

of giant extragalactic HII regions located in the central regions of spiral galaxies.

4. NEW PHOTOMETRY AND COMPLETENESS LIMIT

In Paper II of this series we used the V/V_m test (Schmidt 1968; Sargent 1972; see Paper II) to establish the completeness of our survey. It was then realized that for bright galaxies, the magnitude given by the APM is often far from the one obtained by luminosity profile fitting (see Fig. 1 of Paper I). To palliate this problem we have therefore initiated a program of CCD photometry of the brightest MBGs without accurate magnitude in NED. Galaxies with $B_{APM} < 14.0$ which can be observed from the north latitude were selected. The B,V CCD photometry was acquired at the 1.6 m telescope of the Mont Mégantic, using a THX Thompson 1024×1024 CCD camera. The data were obtained during five nights in October 1993. On each night a number of Landolt's (1992) equatorial standards were concurrently observed to determine the extinction and transformation coefficients. Details of the observations and data reduction can be found in Barnéoud (1994). Total galaxy magnitudes were determined using IRAF aperture photometry package. Table 5 lists the total B and V magnitudes integrated up to the sky level which is reached asymptotically. R_V is the adopted radius, in the V band, where the sky is reached. The uncertainties on B_T and V_T are estimated to be 0.08 and 0.07 respectively. The major contributor to this uncertainty comes from the adoption of the value of the sky brightness (Barnéoud 1994). The last column gives the B–V colors of the galaxies. Nearly all B–V colors are between 0.40 and 0.75. This agrees with the color distribution of non Seyfert Markarian galaxies published by Huchra (1977).

With better estimates of the apparent magnitudes at the bright end, and an increase by 40% in the number of MBGs, we take a second look at the completeness of our survey using the $\langle V/V_m \rangle$ method. For this test, we used the best estimates of B magnitudes of

galaxies: these include 41 galaxies with CCD photometry, 152 galaxies with photoelectric magnitudes and 235 galaxies with APM measured magnitudes. The new results of the V/V_m test are listed in Table 6. The first column gives the absolute magnitude of each interval considered, the second column gives the cumulative number of galaxies up to the absolute magnitude of the interval and the last column gives the cumulative number of galaxies to be added to correct for the incompleteness up to this magnitude. The results are shown in Fig. 3. The error bars correspond to $\sigma = (12N)^{-1/2}$, where N is the number of galaxies (Green 1980). This new test suggests that our survey is complete to $B = 14.7$ and more than 90% complete at $B = 15.0$.

5. THE NATURE OF THE MBGS AND THE ORIGIN OF THE BURSTS

5.1. *Spectroscopic characteristics, redshifts and infrared luminosities*

With the addition of new spectra, we double the number of MBGs that can be classified using diagnostic diagrams. In Fig. 4, we compare the spectral characteristics of our candidates with those of emission-line galaxies from three other samples: the catalogue of HII galaxies (CHIIG; Terlevich *et al.* 1991), a sample of luminous IRAS galaxies (Allen *et al.* 1991) and a sample of compact Kiso galaxies (Comte *et al.* 1994). Fig. 4 illustrates clearly the biases between the different samples. Establishing the boundary between low and high excitation galaxies at $\text{Log}([\text{OIII}]\lambda 5007/\text{H}\beta) = 0.4$ (Coziol 1996), our new data confirm that almost all of the MBGs, and all the IRAS galaxies, are low-excitation SBNGs. The sample of compact Kiso survey seem to contains a slightly higher fraction of HII galaxies. Similarly, Salzer *et al.* (1995) shown that the fraction of low-excitation starbursts detected in the Case survey is also higher than usually found by other prism-objective surveys. These comparison suggests that samples of starburst galaxies suffer various biases which mainly reflect the combination effect of selection criteria and of the magnitude limits

reached by the different surveys. This in particular could explain the bias of the MBG survey towards the SBNGs. In general, HII galaxies have strong emission–lines and high UV–excess, but a relatively faint continuum in B as compared to the SBNGs (Coziol 1996). This is because the SBNGs are located in more massive galaxies with a higher fraction of intermediate aged stellar populations, which dominate in the B band. Because we select our candidates by eye our magnitude limit is relatively bright and we are selecting preferentially galaxies which are more extended and luminous in B. For the same reason, by using a mixed selection criterion, the Case survey is able to detect a higher fraction of low–excitation SBNGs than it would if it was selecting its candidates only based on the presence of emission–lines. Consequently, the deeper magnitude limit reached by the Kiso survey, coupled to its extended definition of UV–excess galaxies allows it to detect a higher fraction of HII galaxies.

In Fig. 4, the continuous curve represents the mean position of standard HII regions. We are using this curve to calibrate our diagnostic diagram in terms of metallicities (see Paper II). The working principle behind our method is explained by the different models of HII regions, which show that the main parameter reproducing this sequence is a variation of the metallicities (McCall *et al.* 1985, hereafter MRS; Dopita & Evans 1986). MRS (1985) have also shown that normal HII regions in the disk of spirals trace a tight distribution around this curve (see their Fig. 3). This could be explained if in general HII regions are ionization–bounded (MRS 1985). In comparison, we can see in Fig. 4 that both the MBGs and the IRAS starbursts are systematically located to the right of our calibration curve. On average, the SBNGs show an excess emission of $[\text{NII}]\lambda 6584$ as compared to normal HII regions. Surprisingly, this phenomenon is not obvious for the compact Kiso galaxies. At the bottom of Fig. 4, we have put the error bars corresponding to 20% uncertainties in the line ratios. Although such uncertainty is compatible with the dispersion of the $[\text{NII}]\lambda 6584/\text{H}\alpha$ ratios, it cannot explain the systematic trend towards higher values. To quantify this

phenomenon, we increased by 0.2 dex the ratio $[\text{NII}]\lambda 6584/\text{H}\alpha$ as predicted by the MRS model. In Fig. 4, the good fit between the shifted MRS model and the data indicates a mean excess of 0.2 dex in the $[\text{NII}]\lambda 6584/\text{H}\alpha$ ratio as compared to normal HII regions.

Excess emission of $[\text{NII}]\lambda 6584$ was already observed before in other samples of emission-line galaxies. It seems like a very common phenomenon in the nucleus of “normal” galaxies (Stauffer 1982). Our observations show now that this is also a characteristic of SBNGs. At the moment, nothing allows us to determine the cause of this phenomenon in the SBNGs. In the literature, various hypotheses have already been suggested. For example, this excess of emission could indicate an overabundance of Nitrogen in the nuclei of galaxies (Stauffer 1982). The same solution was proposed to explain the typical high ratios of $[\text{NII}]\lambda 6584$ in AGNs (Storchi–Bergmann & Pastoriza 1989; Storchi–Bergmann 1991). Considering the possible relation between starburst and AGNs, it would be interesting to know if this overabundance of Nitrogen could have the same origin in both types of galaxies? But this excess of emission could also imply a supplementary source of ionization. All these galaxies may contain an important quantity of hot diffuse gas, which was either shock-ionized by supernovae and stellar winds (Lehnert & Heckman 1994), or even excited by an unresolved weak AGN hidden in their nuclei (Kennicutt *et al.* 1989). Note that these two possibilities are very much similar to the alternatives proposed to explain the nature of LINERs. One could finally suppose that the excess emission of Nitrogen is solely due to selective depletion of cooling elements during dust formation (Shields & Kennicutt 1995). In principle, all these hypothesis could apply to the SBNGs. Depending on the solution however, the nature of the SBNGs would be very much different. The exact cause of the excess emission of Nitrogen in SBNGs seems therefore essential to establish if we want to understand the nature of these objects. The solution to this problem would probably also help us understand what kind of relation could exist between starbursts and AGNs.

The similarities between the spectral characteristics of the MBGs and of the luminous IRAS galaxies suggest that these galaxies have a common nature. In Fig. 5, we compare the redshifts and far-infrared luminosities of the MBGs with those of luminous IRAS galaxies. The sample of IRAS galaxies is composed of the galaxies from the sample of Allen *et al.* (1991) and the sample of luminous infrared galaxies from Veilleux *et al.* (1995). In general, the MBGs possess lower infrared luminosities ($L_{IR} < 10^{11} L_{\odot}$) and are nearer ($z < 0.05$) than the luminous IRAS galaxies. The lower far-infrared luminosities of the MBGs suggests that the MBGs could be starburst galaxies at a different stage of evolution than the luminous IRAS galaxies.

5.2. Morphologies of the SBNGs

In Fig. 6, we present the distribution of the morphologies of the MBGs. Information on the morphologies come from NED or are based on our own CCD imaging (Barnéoud 1994; Barth *et al.* 1995). Only 39% (182) of the MBGs are morphologically classified. Fig. 7 shows that a high fraction of the MBGs are early-type spirals (Sb and earlier). This characteristic is not unique to our sample. In Fig. 6, we show also the distribution of the morphologies of the Markarian galaxies (Mazzarella & Balzano 1986). In this list, the fraction of galaxies which have their morphology classified is similar to ours, although the number of galaxies is almost double (38% or 349 galaxies). The distribution of morphologies of the MBGs and the Markarian galaxies are nearly identical. In Fig. 6, we included also the distribution of the morphologies of the SBNGs as defined by Balzano (1983). As compared to the two other samples, this sample contains a lower fraction of early-type spiral galaxies (earlier than Sa). In paper II, we verified that no difference exists in the intensity of star formation of the early-type MBGs as compared to those of the starbursts in Balzano's sample. The observed bias towards the late-type spirals in this last sample can only be explained

by the particular selection criteria used by this author to define the SBNGs. From our comparison, it is suggested that we should extend the definition of SBNGs in order to include a larger fraction of early-type spirals.

5.3. *The roles of bars and interactions in the SBNGs*

The presence of a nonaxisymmetric feature, like a bar, is frequently suggested to explain a nuclear starburst. Despite the many efforts devoted to this subject however, the current observational evidences are still ambiguous and controversial. For example, using a complete sample of infrared luminous galaxies, Devereux (1994) found that it is in the early-type barred spirals that the nuclear star formation rate is enhanced. This result was contradicted later by Giuricin *et al.* (1994) who suggested that the effect seen by Devereux simply reflects the fact that in early-type spirals the emission is usually more compact than in late-type ones. These authors have also found that it is the late-type barred galaxies that show an enhancement of star formation in their nuclei. In a recent paper, Martin (1995) found that 71% of the galaxies with a nuclear starburst have a strong bar structure, in comparison with 59% for the quiescent galaxies. A quick examination of the Martin's sample clearly show the preponderance of late-type spirals. We may therefore conclude that it is the late-type starburst that are predominantly barred.

In Fig. 6, we distinguished between galaxies with and without a bar. Note that for these statistics we considered SAB as barred. About 35% of the Markarian galaxies and 48% of the MBGs have a bar. This proportion is slightly higher in Balzano's sample, with 58% of barred galaxies. In Fig. 6, it is clearly observed that the frequency of bars detected depends on the morphology of the host galaxy, and increases towards late-type spirals. The fact that Balzano's sample is biased towards the late-type spirals explained therefore the higher fraction of barred galaxies in this sample. With the limited information now

available for our candidates, we cannot say if the variation of the frequency of bar detection as a function of the morphology corresponds to a real effect, or if it means that a bar is more difficult to detect when the galaxy has a strong bulge. Deeper CCD observations or H α imaging of the MBGs will be required to settle this question.

To push our analysis further, we determined the frequency of isolated MBGs with a bar. For this test, we distinguished between early-type starbursts (Sb and earlier) from the late-type starbursts (all spiral types later than Sb). Only 37% of the isolated early-type starbursts have a bar, as compared to 61% for the isolated late-type ones. Note that among the early-type starbursts without a bar, 37% are of type E and SO, as compared to 24% for the Hubble types Sa, Sab and Sb. This suggests that the observational bias effect is marginal. Isolated late-type spirals show a clear tendency to be barred. This result is consistent with those of Giuricin *et al.* (1994) and Martin (1995).

Another popular idea is that massive starbursts occur preferentially within galaxies undergoing interactions. For all the MBGs, we determined the frequency of interacting galaxies by visual inspection of the Palomar and the ESO/SERC atlases. Only 24% (111) of the galaxies in our sample show a clear evidence of interaction. Obviously, this kind of research is limited by the resolution of the plates used. More complete analysis of CCD imaging will be require to detect weak signals of interaction (see Barth *et al.* 1995). Our estimated frequency of interacting MBGs is therefore only a lower limit. This limit is already sufficiently low however to suggest that in a high number of massive galaxies the burst of star formation is probably not solely caused by dynamical processes. In a recent paper, based on a study of HII galaxies, Telles & Terlevich (1995) arrived at exactly this conclusion. According to these authors, only 21% of the HII galaxies show clear signs of interaction. For small mass galaxies, it was suggested that the bursts in the HII galaxies could come from interactions with invisible HI companions (Taylor *et al.* 1993). At

the moment however, this hypothesis is far from being verified (see Taylor *et al.* 1996). Furthermore, for the more massive SBNGs this alternative is even less acceptable. Indeed, it would be difficult to explain the existence of massive HI companions near massive galaxies. Therefore, the tendency towards relative isolation, as suggested by our statistics for the MBGs, should constitute a strong argument in support of the idea that the starburst phenomenon in massive galaxies may also depends on internal mechanisms.

6. SUMMARY AND CONCLUSION

This third installment of the MBG survey brings it to 63% completion. The total list of MBGs amounts now to 469 galaxies brighter than $B_{APM} = 15.5$. New result of the V/V_m test shows that our survey is complete to $B = 14.7$. Our new spectroscopic informations confirm also the bias of our survey towards the low-excitation and metal rich SBNGs. The distribution of morphologies of the MBGs is similar to the one for the Markarian survey and indicates that SBNGs are very common among the early-type spirals (Sb and earlier).

The spectral characteristics of our candidates are similar to those of the luminous IRAS galaxies. But the MBGs are generally nearer ($z < 0.05$) and possess lower infrared luminosities ($L_{IR} < 10^{11} L_{\odot}$) than these galaxies. View the lower infrared luminosities of the MBGs, these galaxies could be starburst galaxies at a different stage of evolution than the luminous IRAS galaxies.

As a common feature with the luminous IRAS galaxies, the MBGs show on average an excess emission of Nitrogen of 0.2 dex as compared to normal disk HII regions. Different mechanisms could produce this effect in the SBNGs and at the moment nothing could allow us to distinguish between the different alternatives. The determination of the exact origin of the excess emission of Nitrogen in SBNGs is essential if we want to understand the nature

of these galaxies. The solution of this problem could probably also help understand what kind of relation could exist between starburst galaxies and AGNs.

Based on the available informations, we are unable to identify one mechanism responsible for the burst of star formation in all the MBGs. This goes contrary to the opinion that starburst in massive galaxies are all produced by interaction. Obvious interacting galaxies constitute only 24% of our candidates. Although this number is only a lower limit, it is sufficiently low to suggest that in some massive galaxies the burst of star formation may depends on internal mechanisms independent of any interaction.

Such internal mechanisms could perhaps be related to a bar. If we consider only the isolated MBGs, we find that the late-type spirals show a clear tendency to be barred. But in our sample, the frequency of bar detection also depends on the morphology of the host galaxy and increases towards the late-type spirals. We cannot tell if this is a real effect or if it is due to the difficulty of detecting bars in early-type galaxies.

Perhaps the origin of the burst is different in starburst galaxies of different morphological types. Bars could be responsible for the enhanced star formation in the nucleus of the late-type spirals, and interactions and mergers could be responsible for the bursts in the early-type galaxies. In these last cases, the bursts should also depend on some self-regulated mechanism, which is necessary to explain the relative isolation of these galaxies.

RC acknowledge the financial support of the Brazilian FAPESP (*Fundação de Amparo à Pesquisa do Estado de São Paulo*), under contract 94/3005–0. The financial support of the Natural Sciences and Engineering Research Council of Canada and the Fonds FCAR du Québec are also gratefully acknowledged. The authors acknowledges the anonymous referee for his comments which have considerably contributed to improve the paper. This research has made use of the NASA/IPAC Extragalactic Database (NED) which is operated by

the Jet Propulsion Laboratory, California Institute of Technology, under contract with the National Aeronautics and Space Administration.

A. Notes on individual objects

00485-0719 Known interacting galaxy, ARP 140.

01056-0449 In a group which includes IC 76 and MRK 973.

01137-5027 Known Sy2 galaxy.

01578-6806 Known emission-line galaxy (Bettoni & Buson 1987).

02043-5525 Known Sy2 galaxy.

03019-2615 This galaxy is not as bright as the B_{APM} would suggest. The total magnitude listed in NED is $B_T = 11.78$. The M_B quoted here, calculated with $B = 8.3$, is thus overevaluated.

03023-2739 This galaxy is also known as HARO 19.

03027-2742 Galaxy pair, the given B_{APM} is just an eye estimate. No magnitude is given in NED.

03540-4229 Arp-Madore interacting galaxy (Sekiguchi & Wolstencroft 1993).

04019-4332 Known Wolf-Rayet galaxy (Conti 1991).

04163-5017 Known Seyfert.

04350-4017 Galaxy pair.

21068-3742 The listed magnitude in NED is $B_T = 13.78$, the magnitude obtained by the APM does not correspond to the whole galaxy. We keep this galaxy because it is obviously brighter than $B = 17$.

21397-5255 Galaxy pair.

22543-3643 The quoted magnitude in NED is $B_T = 10.97$. Our measured magnitude is too bright. The listed M_B is also too bright.

22551-3747 Galaxy pair.

22565-4809 Galaxy pair.

22566-3758 The quoted magnitude in NED is $B_T = 11.84$, the measured magnitude, by the APM does not refer to the whole galaxy. Therefore, our calculated M_B is too faint.

2335-3815 The quoted magnitude in NED is $B_T = 11.51$, the measured magnitude by the APM does not refer to the whole galaxy. Therefore, our calculated M_B is too faint.

23391-3654 Galaxy pair.

REFERENCES

- Allen, D. A., Norris, R. P., Meadows, V. S. & Roche, P. F. 1991, *MNRAS*, 248, 528
- Baldwin, J. A., Phillips, M. M. & Terlevich, R. 1981, *PASP*, 93, 5
- Baldwin, J. A. & Stone, R. P. S. 1984, *MNRAS*, 206, 241
- Balzano, V. A. 1983, *ApJ*, 268, 602
- Barnéoud, R. 1994, Master Thesis, Université de Montréal
- Barth, C. S., Coziol, R. & Demers, S. 1995, *MNRAS*, 276, 1224
- Bettoni, D. & Buson, L. M. 1987, *A&A*, 67, 341
- Comte, G., Augarde, R., Chalabaev, A., Kunth, D. & Maehara, H. 1994, *A&A*, 285, 1
- Conti, P. S. 1991, *ApJ*, 377, 115
- Coziol, R. 1996, *A&A*, 309, 345
- Coziol, R., Barth, C.S. & Demers, S. 1995, *MNRAS*, 276, 2245
- Coziol, R., Demers, S., Peña, M., Torres-Peimbert, S., Fontaine, G., Wesemael, F. & Lamontagne, R. 1993, (Paper I), *AJ*, 105, 35
- Coziol, R., Demers, S., Peña, M. & Barnéoud, R. 1994, (Paper II), *AJ*, 108, 405
- Devereux, N. 1994, in I. Shlosman, ed., *Mass-Transfer Induced Activity in Galaxies*, Cambridge University Press, Cambridge, p. 155
- Dopita, M. A. & Evans, I. N. 1986, *ApJ*, 307, 431
- Gallagher, J. S. 1993, *ASP Conf. Ser. No. 35*, 463
- Giuricin, G., Tamburini, L., Mardirossian, F., Mezzetti M. & Monaco, P. 1994, *ApJ*, 427, 202
- Green, R. F. 1980, *ApJ*, 238, 685

- Huchra, J. J. P. 1977, ApJS, 35, 171
- Kennicutt, R. C., Keel, W. C. & Blaha, C. A. 1989, AJ, 97, 1022
- Landolt, A. U. 1992, AJ, 104, 372
- Lehnert, M. D. & Heckman, T. M. 1994, ApJ, 426, L27
- Martin, P. 1995, AJ, 109, 2428
- Mazzarella, J. M. & Balzano, V. A. 1986, ApJS, 62, 751
- McCall, M. L., Rybski, P. M. & Shields, G.A. 1985, ApJS, 57, 1
- Meurs, E. J. A. & Wilson, A. S. 1984, A&A, 136, 206
- Salzer, J. J., MacAlpine, G. M. & Boroson, T. A. 1989, ApJS, 70, 447
- Salzer, J. J., Moody, J. W., Rosenberg, J. L., Gregory, S. A. & Newberry, M. V. 1995,
AJ109, 2376
- Sargent, W. L. W. 1972, ApJ, 173, 7
- Schmidt, M. 1968, ApJ, 168, 327
- Sekiguchi, K. & Wolstencroft, R. D. 1993, MNRAS, 263, 349
- Shields, J. C. & Kennicutt, R. C. 1995, ApJ, 404, 807
- Stauffer, J. P. 1982, ApJS, 50, 517
- Stone, R. P. S. 1977, ApJ, 218, 767
- Stone, R. P. S. & Baldwin, J. A. 1983, MNRAS, 204, 347
- Storchi-Bergmann, T. S. 1991, MNRAS, 249, 404
- Storchi-Bergmann, T. S. & Pastoriza, M. G. 1989, ApJ, 347, 195
- Takase, B. & Miyauchi-Isobe, N. 1993, PASJ3, 2
- Taylor, C. I., Brinks, E. & Skillman, E. D. 1993, AJ, 105, 128

Taylor, C. I., Brinks, E. & Skillman, E. D. 1996, ApJS, 102, 189

Telles, E. & Terlevich, R. J. 1995, MNRAS, 275, 1

Terlevich, R., Melnick, J., Masegosa, J., Moles, M. & Copetti, M. V. F. 1991, A&A, 91, 285

Veilleux, S. & Osterbrock, D. E. 1987, ApJS, 63, 295

Veilleux, S., Kim, D. -C., Sanders, D. B., Mazarella, J. M. & Soifer, B. T. 1995, ApJ98, 171

Fig. 1.— Spectra of the galaxy MBG22342-2228. a) Blue part of the spectrum centered on $H\beta$. b) Red part of the spectrum centered on $H\alpha$. The wide component of the Balmer lines implies that it is a Seyfert 1.

Fig. 2.— Red spectrum centered on $H\alpha$ of a possible new Seyfert galaxy among our candidates. Based on the absence of obvious large components of the Balmer line, we tentatively classify this galaxy as a Seyfert 2.

Fig. 3.— New V/V_m test for the MBGs. The MBG survey is complete to $B=14.7$

Fig. 4.— Diagnostic diagram of $[OIII]\lambda 5007/H\beta$ vs. $[NII]\lambda 6584/H\alpha$. The long-dashed line is the empirical separation between starbursts and AGNs (Veilleux & Osterbrock 1987). The solid line is the metallicity calibration curve as determined by Coziol *et al.* 1994. The model of MRS (dotted line) was shifted to fit the data for the SBNGs: there is an excess of 0.2 dex in the ratio $[NII]\lambda 6584/H\alpha$ of the SBNGs. The error bars correspond to uncertainties of 20% on the line ratios.

Fig. 5.— Diagram of the far-infrared luminosities as a function of the redshift. The MBGs are compared to the IRAS starburst from Allen *et al.* (1991), and the luminous infrared galaxies from Veilleux *et al.* (1995). The MBGs are less luminous in infrared and closer than the galaxies of these two samples.

Fig. 6.— The morphologies of the MBGs are compared to those of the Markarian galaxies and the SBNGs from Balzano’s sample (1983). The definition of SBNGs, as defined by Balzano, should be enlarged to include a greater number of early-type spirals.

TABLE 1. Third list of UV–bright galaxies.

TABLE 2. Spectroscopic characteristics in the red.

TABLE 3. Spectroscopic characteristics in the blue.

TABLE 4. Metallicities and electron densities of MBGs.

TABLE 5. CCD photometry of selected MBGs.

TABLE 6. Correction for incompleteness.

TABLE 1. Third list of UV-bright galaxies

Name MBG	α (1950)	δ (1950)	B (APM)	$(U - B)$ (APM)	IRAS	M_B (APM)	Cross Identification (NED)	
00336-0347	00 33 36.1	-03 47 48	14.5	+0.2	no	...	MCG-01-02-040	...
00351-0433	00 35 06.7	-04 33 29	14.8	-0.5	no
00405-7400	00 40 30.1	-74 00 33	14.6	-1.3	yes
00407-0655	00 40 45.4	-06 55 01	15.4	-0.5	yes	-18.9
00419-0317	00 41 58.2	-03 17 26	15.4	+0.4	no
00456-0302	00 45 30.2	-03 02 56	11.7	+0.2	yes	-21.8	NGC 259	...
00463-0239	00 46 20.1	-02 39 17	14.7	-0.4	yes	-18.9	MRK 557	...
00476-0527	00 47 37.0	-05 27 58	12.6	-0.5	yes	-21.9	NGC 268	...
00485-0719	00 48 32.8	-07 19 59	13.2*	...	no	-18.6	NGC 275	n
00496-4828	00 49 38.7	-48 28 44	15.3	-0.4	yes	-19.7	ESO 195-IG 010	...
00535-5044	00 53 30.1	-50 44 05	15.5	0.0	yes	-18.5	ESO 195- G 017	...
00550-0516	00 55 02.9	-05 16 20	14.8	-0.4	yes	-19.6	MCG-01-03-041	...
00551-0513	00 55 10.1	-05 13 09	15.3	+0.5	yes	-18.9	MRK 966	...
00556-0631	00 55 38.9	-06 31 49	15.0*	...	no	-19.5	MCG-00-03-050	...
01025-0700	01 02 30.5	-07 00 17	14.9	-0.6	no	...	MCG-01-03-086	...
01046-0416	01 04 37.7	-04 16 34	15.5	-0.1	yes
01047-0324	01 04 42.1	-03 24 15	15.1	-0.3	no	-19.3	MCG-01-03-092	...
01056-0449	01 05 39.5	-04 49 17	15.0	+0.6	yes	n
01069-0307	01 06 53.8	-03 07 11	16.0	-0.6	no	-17.8
01089-4743	01 08 57.9	-47 43 32	15.1	-0.5	yes
01117-6150	01 11 42.7	-61 50 37	15.1	+0.5	no
01137-5027	01 13 47.3	-50 27 11	15.4	+0.2	yes	-18.8	Fairall 294	n
01179-6230	01 17 54.1	-62 30 42	15.4	-0.1	yes	...	AM 0118-623	...
01196-6138	01 19 37.6	-61 38 17	15.0	+0.8	no	...	ESO 113- G 041	...
01196-6201	01 19 38.7	-62 01 33	14.4	0.0	yes	...	ESO 113-IG 043	...
01264-6141	01 26 26.0	-61 41 48	15.3	-0.8	no	...	ESO 113- G 049	...
01366-3010	01 36 41.5	-30 10 42	14.7	+0.3	no	-19.7	NGC 639	...
01400-3330	01 40 00.0	-33 30 42	15.0	-0.3	yes	-19.5	ESO 353- G 033	...
01414-6243	01 41 29.9	-62 43 24	15.0	-0.0	yes	...	ESO 080-IG 004	...
01457-6313	01 45 43.2	-63 13 11	15.6	-0.7	no	-15.9	ESO 080- G 006	...
01578-6806	01 57 53.5	-68 06 43	13.5	-0.4	no	-18.0	NGC 802	n
02043-5525	02 04 20.1	-55 25 54	15.5	+0.6	yes	-19.0	ESO 153-G 020	n
02107-5403	02 10 42.8	-54 03 45	15.4	+0.2	no	-19.4	Fairall 378	...
02204-6450	02 20 24.6	-64 50 14	13.8	0.0	yes	-20.7	ESO 081-G 008	...
02473-5008	02 47 22.6	-50 08 44	14.9	-0.2	yes	...	ESO 199- G 001	...
03012-5803	03 01 15.2	-58 03 22	14.6	+0.4	yes	-19.7	ESO 116-G 005	...
03019-2615	03 01 57.8	-26 15 51	8.3	+1.2	no	-23.4	NGC 1201	n
03023-2739	03 02 23.6	-27 39 15	14.1	+0.2	yes	-20.6	IC 1876,	n
03027-2742	03 02 46.6	-27 42 24	15.0*	...	yes	...	ESO 417-IG 014	n
03031-4907	03 03 09.1	-49 07 27	15.5	-1.1	yes	...	ESO 199-IG 015	...

TABLE 1. (continued)

Name MBG	α (1950)	δ (1950)	B (APM)	$(U - B)$ (APM)	IRAS	M_B (APM)	Cross Identification (NED)	
03037-2725	03 03 44.1	-27 25 24	15.4	+0.4	yes	...	ESO 480- G 030	...
03118-5732	03 11 48.7	-57 32 38	14.0	-0.7	yes	-16.9	ESO 116- G 012	...
03142-2602	03 14 12.0	-26 02 17	14.9	+0.3	no	...	MCG-04-08-055	...
03169-0618	03 16 57.8	-06 18 08	14.4	-0.2	yes	-18.0	MRK 1075	...
03278-0424	03 27 49.4	-04 24 48	13.2	+0.2	yes	-22.0	KUG 0327-044	...
03301-0455	03 30 07.7	-04 55 09	13.7	+0.3	yes	...	KUG 0330-049	...
03383-0359	03 38 19.1	-03 59 24	15.1	+0.2	yes	-18.6	MRK 1078	...
03400-0427	03 40 03.1	-04 27 27	13.7	+0.7	yes	...	IC 347	...
03402-0632	03 40 12.6	-06 32 24	14.3	+0.4	yes	-20.4	MRK 1191	...
03458-0646	03 45 57.7	-06 46 45	15.2	+0.3	yes	...	MCG-01-10-038	...
03505-4440	03 50 31.0	-44 40 52	13.6	-0.8	yes	-18.2	NGC 1476	...
03533-2817	03 53 18.6	-28 17 01	13.7*	...	yes	-17.8	IC 2007	...
03540-4229	03 54 01.1	-42 29 49	11.9*	0.0	yes	-18.3	NGC 1487	n
03540-2636	03 54 04.3	-26 36 58	13.8	+0.2
03590-4910	03 59 02.4	-49 10 08	13.6	-1.0	yes	...	ESO 201- G 014	...
04000-5250	04 00 00.7	-52 50 49	15.5	+0.7	yes	-20.1	IC 2028	...
04019-4332	04 01 54.1	-43 32 11	12.9	-0.7	yes	-17.7	NGC 1510	n
04022-4329	04 02 15.6	-43 29 06	11.5	+0.4	yes	-18.9	NGC 1512	...
04026-3618	04 02 36.0	-36 18 38	15.1*	...	no	-16.3	ESO 359- G 016	...
04030-4610	04 03 02.4	-46 10 38	15.0	0.0	no	-16.2	ESO 250- G 005	...
04048-5248	04 04 51.2	-52 48 12	13.6	-1.0	yes	-16.2	NGC 1552	...
04074-4538	04 07 28.3	-45 38 52	10.4	+0.4	yes	-21.0	IC 2035	...
04098-4608	04 09 49.6	-46 08 05	14.1	-0.8	yes	-20.0	AM 0409-460	...
04100-3258	04 10 03.9	-32 58 42	10.6	...	no	-20.0	NGC 1531	...
04100-3301	04 10 05.6	-33 01 24	13.4	-1.5	yes
04101-3300	04 10 08.8	-33 00 04	11.2	+2.7	yes	-19.8	NGC 1532	...
04139-5104	04 13 58.1	-51 04 12	15.6	-0.9	yes	-17.9	ESO 201-IG 026	...
04163-5017	04 16 23.3	-50 17 08	11.3	-0.3	yes	-19.4	NGC 1556	n
04189-5503	04 18 53.5	-55 03 24	10.6	+2.6	yes	-20.9	NGC 1566	...
04210-4042	04 21 01.1	-40 42 59	14.2	+0.3	yes	-20.3	NGC 1572	...
04243-4323	04 24 23.4	-43 23 05	15.0	-0.2	yes
04253-5317	04 25 22.3	-53 17 55	14.5	-0.1	yes	-19.1	IC 2073	...
04259-4216	04 25 54.7	-42 16 28	13.0	-0.9	yes	-21.0	NGC 1585	...
04267-5510	04 26 45.3	-55 10 07	15.1	-1.0	no	...	ESO-LV 1570321	...
04268-4321	04 26 52.9	-43 21 02	14.6	-0.5	yes
04287-5148	04 28 44.1	-51 48 21	15.0	+0.5	yes	-16.5
04309-4947	04 30 55.9	-49 46 52	15.4	-0.5	yes	-16.6	ESO 202- G 035	...
04337-4218	04 33 42.7	-42 18 17	15.0	-0.4	yes	...	ESO 304- G 002	...
04341-4035	04 34 11.3	-40 35 38	15.5	-0.2	yes
04350-4017	04 35 02.7	-40 17 58	15.5	-0.6	yes	...	ESO 304-IG 005	n

TABLE 1. (continued)

Name MBG	α (1950)	δ (1950)	B (APM)	$(U - B)$ (APM)	IRAS	M_B (APM)	Cross Identification (NED)	
04425-4135	04 42 33.6	-41 35 20	14.4	0.0	yes	...	NGC 1660	...
04435-4140	04 43 30.0	-41 40 09	14.8	+0.9	no	...	ESO 304- G 019	...
20533-4410	20 53 23.0	-44 10 44	14.6	-0.2	yes	-19.5	NGC 6983	...
21035-2436	21 03 30.9	-24 36 48	15.0	+0.4	yes	...	NGC 7019	...
21065-4543	21 06 32.0	-45 43 54	14.9	+0.3	yes	...	AM2106-454	...
21068-3742	21 06 51.2	-37 42 04	17.0	+0.1	yes	...	ESO 342-IG 013	n
21097-3804	21 09 47.5	-38 04 32	15.4	-1.3	yes	-20.8	ESO 342- G 022	...
21117-4724	21 11 45.3	-47 24 44	15.4	+0.5	yes	-18.7	NGC 7038	...
21118-4701	21 11 49.9	-47 01 51	15.0	-0.2	no	-20.8	Fairall 961	...
21142-2319	21 14 13.8	-23 19 52	15.0	+0.9	no	...	ESO 530- G 029	...
21169-2224	21 16 56.7	-22 24 09	14.5	...	no	...	ESO 599- G 007	...
21194-3653	21 19 25.7	-36 53 42	14.5	+0.6	yes	-18.4	ESO 402- G 026	...
21273-4439	21 27 21.0	-44 39 00	14.9	-0.2	yes	-20.9	ESO 287-IG 030	...
21317-5627	21 31 46.1	-56 27 30	15.2	+0.3	yes	-21.2	AM 2131-562	...
21331-5446	21 33 06.5	-54 46 07	11.3*	...	yes	-19.0	NGC 7090	...
21384-5300	21 38 25.8	-53 00 06	12.3	-1.8	yes	...	IC 5125	...
21397-5255	21 39 42.8	-52 55 10	15.2	-0.3	yes	-19.0	ESO 188-IG 018	n
21449-5512	21 44 56.8	-55 12 13	15.4	+0.2	no	-20.7	Fairall 591	...
21456-6056	21 45 37.0	-60 56 45	14.3	+0.2	yes	-18.8	NGC 7125	...
21488-5548	21 48 49.1	-55 48 17	14.7	-0.2	yes	-18.3	NGC 7140	...
21509-1331	21 50 59.4	-13 31 53	15.2	+0.2	no	...	NPM16-13.054	...
21515-6023	21 51 31.3	-60 23 59	15.5	-0.1	no
22051-5741	22 05 10.8	-57 41 16	13.5	+1.7	yes	-18.3	NGC 7205	...
22198-3227	22 19 50.6	-32 27 08	15.1	+1.0	no	-20.1	ESO 467- G 046	...
22215-3356	22 21 33.4	-33 56 24	12.9*	...	yes	-20.3	NGC 7267	...
22220-3134	22 22 00.1	-31 34 47	14.8	+1.3	no	-20.4	ESO 467- G 054	...
22228-3127	22 22 50.4	-31 27 19	15.0	+0.5	no	...	NGC 7268	...
22233-3123	22 23 20.7	-31 23 59	13.8	+0.6	yes	-19.9	NGC 7277	...
22312-3239	22 31 12.0	-32 39 18	15.4	+0.5	yes	-18.0	ESO 405- G 029	...
22333-3159	22 33 21.8	-31 59 13	15.0	+1.1	no	-20.1	ESO 468- G 016	...
22467-4906	22 46 42.4	-49 06 51	15.1	+0.4	yes	-21.1	Fairall 358	...
22474-5142	22 47 26.6	-51 42 47	15.5	-0.2	yes
22514-3721	22 51 27.4	-37 21 03	15.1	-0.3	no	...	ESO 406- G 018	...
22522-3851	22 52 17.6	-38 51 05	15.2	0.0	yes	-17.6	ESO 346- G 014	...
22530-3427	22 53 05.2	-34 27 35	14.8	-0.4	yes	-20.5	ESO 406- G 021	...
22530-3449	22 53 05.8	-34 49 22	13.7	-0.6	no	-22.9	ESO 406- G 022	...
22538-3702	22 53 53.5	-37 02 26	14.7	-0.6	yes	-17.5	NGC 7418A	...
22543-3643	22 54 23.0	-36 43 49	8.6	+2.1	yes	-23.2	IC 1459	n
22548-3421	22 54 48.8	-34 21 21	14.6	+0.3	no	...	AM 2254-342	...
22550-3607	22 55 05.0	-36 07 42	13.0*	...	no	-18.7	IC 5270	...

TABLE 1. (continued)

Name MBG	α (1950)	δ (1950)	B (APM)	$(U - B)$ (APM)	IRAS	M_B (APM)	Cross Identification (NED)	
22551-3747	22 55 08.8	-37 47 06	15.2	-0.8	no	...	ESO 346-IG 020	n
22565-4809	22 56 32.1	-48 09 34	14.4	-1.0	yes	...	ESO 239-IG 006	n
22566-3758	22 56 39.0	-37 58 43	15.4	-0.9	yes	-15.4	IC 5273	n
22580-3538	22 58 01.8	-35 38 23	14.8	-0.8	yes	-17.1	IC 5269C	...
23004-3540	23 00 27.4	-35 40 26	15.2	-0.4	no
23164-6128	23 16 28.2	-61 28 58	14.5	0.0	yes	...	ESO 148- G 004	...
23283-6112	23 28 20.9	-61 12 30	14.3	+0.2	yes	-18.9	ESO 148- G 018	...
23289-6253	23 28 56.8	-62 53 49	15.5	+0.1	no
23335-3812	23 33 35.6	-38 12 54	14.4	+0.5	no	-15.4	NGC 7713	n
23336-6333	23 33 37.3	-63 33 57	15.5	-0.1	yes
23361-5208	23 36 07.4	-52 08 15	14.7	-0.7	yes	-17.2	ESO 240- G 012	...
23391-3654	23 39 11.1	-36 54 11	15.4	-0.4	no	...	ESO 408-IG 017	n
23417-3608	23 41 45.7	-36 08 08	15.5	+0.1	no
23473-6336	23 47 21.5	-63 36 19	14.5	-0.2	yes	...	AM 2347-633	...
23493-6324	23 49 21.2	-63 24 42	15.3	-0.1	yes	...	AM 2349-632	...

*Galaxy not in the APM file, B magnitude taken from NED.

TABLE 6. Correction for incompleteness

Limiting Magnitude	No. of galaxies	$\langle V/V_m \rangle$	Galaxies added
13.20	23	0.520	...
13.40	28	0.495	...
13.60	42	0.542	...
13.80	56	0.522	...
14.00	74	0.515	...
14.20	99	0.512	...
14.30	111	0.496	...
14.40	129	0.503	...
14.50	149	0.507	...
14.60	173	0.512	...
14.70	199	0.510	...
14.80	215	0.482	4
14.90	240	0.474	14
15.00	267	0.467	29
15.10	288	0.446	64
15.20	312	0.432	94
15.30	340	0.423	114
15.40	374	0.422	145
15.50	401	0.407	205
15.60	416	0.375	285
15.70	421	0.334	385
15.80	425	0.297	515
15.90	428	0.264	635